NUCL SCI TECH (2016) 27:36
DOI 10.1007/s41365-016-0043-4

Improvement on application of Dancoff factor and resonance interference table

Yu Han[1] · Xiao-Feng Jiang [2] · De-Zhong Wang[1]

Received: 11 February 2015 / Revised: 5 April 2015 / Accepted: 24 April 2015 / Published online: 11 April 2016

Abstract An improvement for application of Dancoff factor is developed. It combines Stamm'ler's two-term method for resonance integral calculation with neutron current method for Dancoff factor calculation. Stamm'ler's formulation, which is originally derived for the infinite lattice geometry, can be easily revised to contain the Dancoff factor explicitly, while the neutron current method can easily calculate the Dancoff factor for general irregular assembly geometry. For the resonance interference effects, the resonance interference factor table is built in pairs of nuclides, only for the interference between ^{238}U and other resonance nuclides, spanning over a range of background cross-section and number density ratio of the pairing nuclides. A series of verification calculations have been carried out for problems of infinite lattice and single assembly geometry, with two or multiple resonance absorbers. For these verification calculations, our improvement on Dancoff factor application and resonance interference give good results.

Keywords Resonance · Self-shielding · Equivalence theory · Dancoff factor · Neutron current method · Stamm'ler's method · Resonance interference effect · Resonance interference factor

✉ Yu Han
hanyu19841203@hotmail.com

[1] School of Nuclear Science and Engineering, Shanghai Jiaotong University, Shanghai 200240, China

[2] Shanghai NuStar Nuclear Power Technology Co., Ltd., Shanghai 200000, China

1 Introduction

The conventional method of evaluating effective resonance cross-section is based on the equivalence theory, which turns the effect from moderator in heterogeneous models into the escape cross-section. Under equivalence theory, the background cross-section for heterogeneous models can be divided into two parts, one from the homogeneous medium and another from the escape cross-section. Stamm'ler's method [1, 2], which is an equivalence theory method built on Carlvik's two-term rational approximation, is originally derived for the case of infinite lattice geometry, making use of first-flight collision probability and transmission probability. Another equivalent theory method, the Dancoff method, applies the Dancoff factor directly to the escape cross-section of an isolated fuel rod surrounded with infinite moderator. It is derived by using either Wigner's one-term rational approximation or by taking the limit of infinite absorption. The Dancoff method is easier to apply in general as it involves only the calculation of Dancoff factor, while the Stamm'ler's method is difficult to apply to cases of non-lattice geometry, though it is more accurate than the Dancoff method.

Sugimura and Yamamoto [3] developed the neutron current method to calculate in a easy way the Dancoff factor for irregular assembly geometry, which requires only a fixed source transport calculation with "black" fuel rods.

In this paper, we propose to rewrite the Stamm'ler equations so that the Dancoff factor appears there explicitly. The neutron current method can then be used to calculate the Dancoff factor for irregular assembly geometry and to apply it to the Stamm'ler equations. The method of

characteristics [4] is applied to the fixed source transport calculation in the limit of black fuel rods.

When the multi-group cross-section library is generated, the resonance cross-section does not include the interference effect between different kinds of absorbers. In reality, there are always multiple resonance nuclides, especially with burnup of the fuel, the presence of the additional resonances will exaggerate the spectral flux dips and change the results in calculation. In common practice, the background cross-section iteration method [5, 6] is often used to correct the interference effects. But the iteration method is crude and not very effective.

In more recent methods of lattice calculation, the resonance interference effect among different resonance absorbers can be taken into account by resonance interference factors (RIFs) [7, 8], which are calculated and tabulated before evaluating the effective cross-section, and used as correction multipliers to the effective cross-section.

In the presented paper, a simplified evaluation of resonance interference factor table is done. For a typical reactor design, ^{238}U dominants the number density of the resonance absorbers. So the interference effect between any two resonance absorbers other than ^{238}U can be ignored for simplicity. The RIFs between ^{238}U and another resonance nuclide are tabulated for different background cross-sections and different number density ratios.

The theoretical considerations are discussed in detail in Sect. 2 and verified in Sect. 3 for problems of infinite lattice geometry and single assembly geometry, with two or multiple resonance absorbers. The results for the case of infinite lattice geometry with only two resonance absorbers, for the case with multiple resonance absorbers, and for the case of single assembly geometry, are given.

2 Theory

The neutron slowing-down equation, the Stamm'ler's method, and the Yamamoto's neutron current method are briefly reviewed and summarized in Sects. 2.1–2.3. In Sect. 2.4, we discuss how to apply Yamamoto's Dancoff factor calculation to Stamm'ler's method of resonance integral calculation. The simplified RIF table is discussed in Sect. 2.5. Finally, Sect. 2.6 describes the overall calculation procedure for implementing the improvement.

2.1 Neutron slowing-down equation

For an isolated fuel rod, the neutron slowing-down equation is:

$$\sum_{\mathrm{t,f}}(E)\phi_{\mathrm{f}}(E)V_{\mathrm{f}} = V_{\mathrm{f}}P_{\mathrm{ff}}(E)\int_{E}^{E/\alpha_{\mathrm{f}}}\frac{\sum_{\mathrm{s,f}}(E')\phi_{\mathrm{f}}(E')}{(1-\alpha_{\mathrm{f}})E'}\mathrm{d}E' + V_{\mathrm{m}}P_{\mathrm{m0}}(E)\int_{E}^{E/\alpha_{\mathrm{m}}}\frac{\sum_{\mathrm{s,m}}(E')\phi_{\mathrm{m}}(E')}{(1-\alpha_{\mathrm{m}})E'}\mathrm{d}E', \tag{1}$$

where $\alpha = [(a-1)/(a+1)]2$; a is mass number of the nuclide; $\sum_{\mathrm{t,f}}(E)$ is total cross-section in fuel region; $\sum_{\mathrm{s,f}}(E)$ and $\sum_{\mathrm{s,m}}(E)$ are scattering cross-section in fuel and moderator region, respectively; $\phi_{\mathrm{f}}(E)$ and $\phi_{\mathrm{m}}(E)$ are flux in fuel and moderator region, respectively; $P_{\mathrm{ff}}(E)$ is first-flight collision probability in the fuel region; $P_{\mathrm{m0}}(E)$ is first-flight escape probability in the moderator region; V_{f} is volume of fuel region and V_{m} is volume of moderator region.

In moderator region, assuming that the $1/E$ spectrum is suitable and $\sum_{\mathrm{s,f}}(E)$ is constant in the integral, the second term on the right part in Eq. (1) can be simplified. And assuming that the absorption cross-section in moderator is negligible, total cross-section is equal to the scattering cross-section. Substituting the reciprocity relationship of Eq. (2) into Eq. (1) and using some approximation, the neutron spectrum can be solved as Eq. (3).

$$\sum_{\mathrm{t,f}}V_{\mathrm{f}}(1-P_{\mathrm{ff}}(E)) = \sum_{\mathrm{t,m}}(E)V_{\mathrm{m}}P_{\mathrm{m0}}(E), \tag{2}$$

$$\phi_{\mathrm{f}}(E) = \frac{\lambda P_{\mathrm{ff}}\sum_{\mathrm{p,f}} + (1-P_{\mathrm{ff}})\sum_{\mathrm{t,f}}}{\sum_{\mathrm{t,f}} - (1-\lambda)P_{\mathrm{ff}}\sum_{\mathrm{p,f}}}\cdot\frac{1}{E}, \tag{3}$$

where λ is the Goldstein–Cohen factor, with $\lambda = 1$, $\lambda = 0$ and $0 < \lambda < 1$ being the narrow, wide and intermediate resonance approximation, respectively.

If the $P_{\mathrm{ff}}(E)$ in isolated fuel rod is replaced with the first-flight collision probability in a lattice model, $P_{\mathrm{FF}}(E)$, the neutron spectrum in the lattice model can be written as:

$$\phi_{\mathrm{f}}(E) = \frac{\lambda P_{\mathrm{FF}}\sum_{\mathrm{p,f}} + (1-P_{\mathrm{FF}})\sum_{\mathrm{t,f}}}{\sum_{\mathrm{t,f}} - (1-\lambda)P_{\mathrm{FF}}\sum_{\mathrm{p,f}}}\cdot\frac{1}{E}. \tag{4}$$

2.2 Stamm'ler's method for evaluating the effective cross-section

In an infinite lattice system, according to 0's method, the $P_{\mathrm{FF}}(E)$ and $P_{\mathrm{ff}}(E)$ can be correlated as:

$$P_{\mathrm{FF}} = P_{\mathrm{ff}} + \frac{x(1-P_{\mathrm{ff}})^2}{x(1-P_{\mathrm{ff}}) + A}, \tag{5}$$

where $A = S_{\mathrm{b}}\gamma_{\mathrm{b}}^0/(S_{\mathrm{f}}t_{\mathrm{fb}}^2)$, S_{b} is surface area of cell boundary, S_{f} is surface area of fuel lump, γ_{b}^0 is blackness of the cell at $\sum_{\mathrm{t,f}} = 0$, and t_{fb} is transmission probability that neutrons leaving a fuel surface with cosine angular distribution will

reach the cell boundary; $x = \sum_{t,f} / \sum_e$, $\sum_e = S_f/(4V_f)$, V_f is volume of fuel lump.

The expression of P_{ff} in Carlvik's two-term rational approximation is as follows:

$$P_{ff} = x\left(\frac{2}{x+2} - \frac{1}{x+3}\right). \tag{6}$$

Substituting Eq. (6) into Eq. (5), we have the expression of P_{FF} with two-term rational approximation:

$$P_{FF} = x\left[\frac{\beta_1}{x+\alpha_1} + \frac{\beta_2}{x+\alpha_2}\right], \tag{7}$$

where $\alpha_{1,2} = (5A+6)(A^2+36A+36)/[2(A+1)]$, $\beta_1 = [(4A+6)/(A+1) - \alpha_1]/(\alpha_2 - \alpha_1)$, and $\beta_2 = 1 - \beta_1$.

Substituting Eq. (7) into Eq. (4), and assuming that $(1-\lambda)\sigma_{s,F}$ is far smaller than $\sigma_{t,F}$, we have:

$$\phi_f(E) = \sum_{n-1}^{2} \beta_n \left[\frac{\lambda\sigma_{p,f} + \alpha_n\sigma_e}{\sigma_{\alpha,f}(E) + \lambda\sigma_{rs,f}(E) + \lambda\sigma_{p,f} + \alpha_n\sigma_e}\right]\frac{1}{E}, \tag{8}$$

Equation (9) defines effective cross-section of a single resonance nuclide in group g. Substituting Eq. (8) into Eq. (9) and assuming $\lambda\sigma_{rs,f}(E)$ is far smaller than $\sigma_{\alpha,f}(E)$, too, the effective cross-section can be defined by Eq. (10):

$$\sigma_{x,g} = \frac{\int_{\Delta E_g} \sigma_x(E)\phi_f(E)\mathrm{d}E}{\int_{\Delta E_g} \phi_f(E)\mathrm{d}E}, \tag{9}$$

$$\sigma_{x,g} = \frac{RI_{1,x} + RI_{2,x}}{\Delta u_g - \frac{RI_{1,\alpha}}{\sigma_{b1}} - \frac{RI_{2,\alpha}}{\sigma_{b2}}}, \tag{10}$$

where $RI_{n,x} = \beta_n F_x(\sigma_{bn})$, $\sigma_{bn} = \lambda\sigma_{p,f} + \alpha_n\sigma_e$, $F_x(\sigma_{bn}) = \int_{\Delta E_g} \frac{\sigma_{bn}\sigma_{x,f}(E)}{\sigma_{\alpha,f}(E)+\sigma_{bn}} g\frac{dE}{E}$, and $\Delta u_g = \int_{\Delta E_g} \frac{dE}{E}$.

In Eq. (10), Δu_σ is usually adjusted to unity by the library. The resonance integral $F_x(\sigma_{bn})$ will be determined by the interpolation in the resonance integral table which will be supplied by the nuclear data library. Therefore, to evaluate the effective cross-section, parameter A in Stamm'ler's method is calculated in advance. In the original Stamm'ler's derivation, A is a characteristic constant for a given infinite lattice problem and is evaluated by using collision probability method. Instead of using the collision probability method to calculate A, we will relate A to Dancoff factor and then use Yamamoto's neutron current method to calculate the Dancoff factor in a simple way, which is valid even for the non-lattice assembly geometry.

2.3 The neutron current method for calculating Dancoff factor

According to Eq. (4), the total reaction rate can be written as:

$$R_{tot}(E) = \sum_{t,f}(E)\phi_f(E) = \frac{\sum_{t,f}(E)}{\sum_{t,f}(E) - (1-\lambda)P_{FF}(E)\sum_{p,f}} \times \left[\lambda P_{FF}(E)\sum_{p,f} + (1 - P_{FF}(E))\sum_{t,f}(E)\right]. \tag{11}$$

Taking the black-limit of very large total cross-section, the limit of Eq. (11) can be expressed as:

$$\lim_{\sum_{t,f}\to\infty} R_{tot} = \lim_{\sum_{t,f}\to\infty}\left(\lambda P_{FF}\sum_{p,f} + (1-P_{FF})\sum_{t,f}\right). \tag{12}$$

In the black-limit, Wigner's one-term rational approximation to P_{FF} is valid:

$$P_{FF} = \frac{x}{x+D}. \tag{13}$$

Substituting Eq. (12) into Eq. (13), we have:

$$\lim_{\sum_{t,f}\to\infty} R_{tot} = \lambda\sum_{p,f} + D\sum_{e}. \tag{14}$$

If the total cross-section is large enough, the total reaction rate is very close to Eq. (14). So when the total reaction rate in the resonance region is obtained by Yamamoto's fixed source transport calculation in the limit of large total cross-section, the Dancoff factor can be calculated by:

$$D = \frac{R_{tot} - \lambda\sum_{p,f}}{\sum_e}. \tag{15}$$

In using the Dancoff method for effective resonance cross-section calculation, the Dancoff factor from Eq. (15) is applied directly to the equivalent escape cross-section of an isolated rod to calculate the background cross-section for resonance integral table lookup. Instead, we propose to apply the Dancoff factor from Eq. (15) to the Stamm'ler's method equations.

2.4 Application of Dancoff factor to Stamm'ler's method

An alternative equivalent definition of Dancoff factor is given as [2, 3]:

$$D = \lim_{\sum_{t,f}\to\infty} \frac{1 - P_{FF}}{1 - P_{ff}}. \tag{16}$$

Also note that the first-flight collision probability satisfies the following relation:

$$\lim_{\sigma_{t,f}\to\infty} x(1 - P_{ff}) = 1. \tag{17}$$

Substituting Eqs. (5) and (17) into Eq. (16), the relationship between the Dancoff factor and the parameter A in Stamm'ler's method is obtained:

$$D = \frac{A}{1+A}, \quad \text{or} \quad A = \frac{D}{1-D}. \tag{18}$$

Therefore, the neutron current method can be used to calculate D and thus obtain A without having to use the collision probabilities in Eq. (5). Furthermore, the neutron current method is applicable to the general non-lattice assembly geometry. Once A is known, the two-term coefficients in Eq. (7) can be calculated. The Stamm'ler's method can then be used without any change to calculate the effective cross-section by Eq. (10).

2.5 Simplification of the resonance interference factor table

Traditionally the background cross-section iteration method is used for the resonance interference correction, but the iteration method is not yet effective. A method using simplified resonance interference factor (RIF) table is given below.

In a typical LWR core, the number density of ^{238}U is usually much larger than that of other resonance nuclides. The spectrum in the resonance region is dominated by resonance absorption from ^{238}U. To simplify the resonance interference treatment, only the interference effects between ^{238}U and other resonance nuclides are considered. To correct the resonance overlap (interference) effects, the resonance interference factors (RIFs) prepared with Eq. (19) are used.

$$\mathrm{RIF}_x^{238\to i}(\sigma_{\mathrm{b},i}, N_i/N_{238}) = \frac{\sigma_{x,i}^{\mathrm{eff}}(\sigma_{\mathrm{b},i}, N_i/N_{238})}{\sigma_{x,i}^{\mathrm{eff}}(\sigma_{\mathrm{b},i}, 0)}, \tag{19}$$

where $\sigma_{x,i}^{\mathrm{eff}}(\sigma_{\mathrm{b},i}, 0)$ is effective cross-section for nuclide i and reaction type x, at zero number density of ^{238}U, and background cross-section $\sigma_{\mathrm{b},i}$; $\sigma_{x,i}^{\mathrm{eff}}(\sigma_{\mathrm{b},i}, N_i/N_{238})$ is effective cross-section for nuclide i and reaction type x, at a ratio of number density of N_i/N_{238}, and background cross-section $\sigma_{\mathrm{b},i}$; $\mathrm{RIF}_x^{238\to i}(\sigma_{\mathrm{b},i}, N_i/N_{238})$ is resonance interference factor from ^{238}U to nuclide i and reaction type x, at number density ratio N_i/N_{238}, and background cross-section $\sigma_{\mathrm{b},i}$.

Corresponding to the overlap effects from ^{238}U to other resonance nuclides, the interference effects from other resonance nuclides to ^{238}U at the same number density ratio (N_i/N_{238}) are calculated by Eq. (20):

$$\mathrm{RIF}_x^{i\to 238}(\sigma_{\mathrm{b},238}, N_i/N_238) = \frac{\sigma_{x,238}^{\mathrm{eff}}(\sigma_{\mathrm{b},238}, N_i/N_{238})}{\sigma_{x,238}^{\mathrm{eff}}(\sigma_{\mathrm{b},238}, 0)}. \tag{20}$$

Taking ^{238}U as an example, the whole process of evaluating a resonance interference factor is described below.

For $\sigma_{x,238}^{\mathrm{eff}}(\sigma_{\mathrm{b},238}, 0)$, a calculation through solving the slowing-down equation is done by RMET21 [9], in which only ^{238}U and hydrogen are present. The background cross-section is defined as:

$$\sigma_{\mathrm{b},238} = \lambda_{238}\sigma_{\mathrm{p},238} + \frac{N_{\mathrm{H}}}{N_{238}}\lambda_{\mathrm{H}}\sigma_{\mathrm{p,H}}. \tag{21}$$

The number density of ^{238}U will be set to unity for convenience. To get different background cross-sections, we just need to adjust the number density of Hydrogen.

For $\sigma_{x,i}^{\mathrm{eff}}(\sigma_{\mathrm{b},i}, N_i/N_{238})$, the calculation is done by RMET21 in presence of ^{238}U, hydrogen, and nuclide i. The background cross-section is defined as:

$$\sigma'_{\mathrm{b},238} = \lambda_{238}\sigma_{\mathrm{p},238} + \frac{N_i}{N_{238}}\lambda_i\sigma_{\mathrm{p,i}} + \frac{N_{\mathrm{H}}}{N_{238}}\lambda_{\mathrm{H}}\sigma_{\mathrm{p,H}}, \tag{22}$$

where $\sigma_{\mathrm{b},238}$ and $\sigma'_{\mathrm{b},238}$ are effective cross-section for nuclide i, group g, and resonance reaction type x, without and with resonance overlap correction, respectively. In Eq. (22), the value of N_i/N_{238} will cover the possible range in a typical LWR. To make $\sigma'_{\mathrm{b},238}$ equal $\sigma_{\mathrm{b},238}$, we just need to adjust the number density of hydrogen.

When the effective cross-sections with and without the interference effect are obtained, RIF from resonance nuclide i to ^{238}U is calculated by Eq. (20). For a typical lattice, the flux spectrum varies with the background cross-section, caused by different number densities of ^{238}U or different shielding conditions. So, a series of calculations

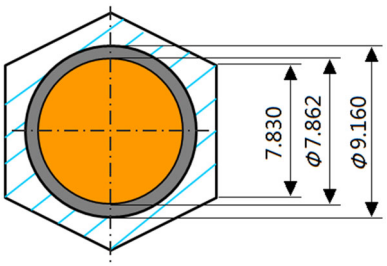

Fig. 1 Cell geometry for infinite lattice calculation

Table 1 Description of two calculation methods

Methods	Stamm'ler's method	Improved use of Dancoff factors	Treatment of resonance interference	
			Iteration	RIFs
A		√	√	
B		√		√
C	√		√	

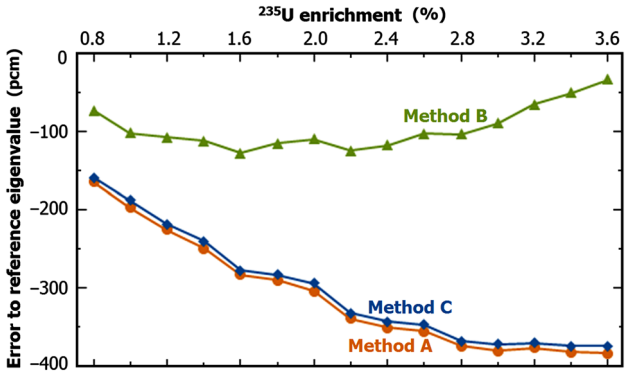

Fig. 2 Error to reference eigenvalue as a function of ^{235}U enrichment for the two absorbers case

with different background cross-sections and different number density ratios are carried out.

For resonance nuclides other than ^{238}U, the effective cross-section for a specific resonance nuclide without the resonance interference correction is calculated by interpolating the nuclear data library, before interpolating the RIFs table to obtain RIF. Finally, the RIF is multiplied to the uncorrected effective cross-section as:

$$\sigma'_{x,i,g} = \mathrm{RIF}^{238\to i}_{x,g} \cdot \sigma_{x,i,g}, \tag{23}$$

where $\mathrm{RIF}^{238\to i}_{x,g}$ is resonance interference factor for nuclide i, group g, and resonance reaction type x.

For ^{238}U, the resonance interference effects from other resonance nuclides to ^{238}U are counted into the correction as:

$$\sigma'_{238,x,g} = \left(\prod_{i'} \mathrm{RIF}^{i'\to 238}_{x,g}\right) \cdot \sigma_{238,x,g}, \tag{24}$$

where $\Pi_{i'}\mathrm{RIF}^{i'\to 238}_{x,g}$ is cumulative product of resonance interference factors from all resonance nuclides to ^{238}U.

2.6 Calculation procedure

The calculation procedures for implementing the improvement are described as follows.

1. Prepare table of RIFs as described in Sect. 2.5.

Table 2 Micro-cross-section and relative error in absorption and neutron production for ^{235}U of 1.8 % inrichment and ^{238}U in Case-A

Energy groups	Absorption of ^{235}U			Neutron production of ^{235}U			Absorption of ^{238}U		
	$\sum^{a}$	$\delta(\%)^{b}$		$\sum^{a}$	$\delta(\%)^{b}$		$\sum^{a}$	$\delta(\%)^{b}$	
		Method A	Method B		Method A	Method B		Method A	Method B
15	4.4904	0.02	0.02	7.9300	0.05	0.04	0.69442	−0.19	−0.17
16	5.6824	−0.12	−0.10	10.420	−0.12	−0.09	0.73277	−0.81	−0.78
17	6.9880	−0.23	−0.17	12.586	−0.22	−0.22	0.94726	−1.65	−1.60
18	9.5619	−0.04	0.17	14.984	−0.34	0.11	0.87767	−1.62	−1.56
19	12.184	−0.69	−0.11	19.408	−1.07	−0.08	1.1712	−1.75	−1.71
20	16.946	−0.2	0.25	28.906	−0.13	0.43	1.3449	−2.29	−2.26
21	27.897	−0.36	−1.07	45.743	−1.06	−0.76	1.5361	−0.03	0.05
22	34.768	−0.37	−0.18	53.527	−0.12	−0.51	2.4168	0.06	0.08
23	58.251	−2.36	0.55	99.149	−2.75	0.58	2.1192	−0.71	0.12
24	69.201	−3.37	−0.01	102.82	−2.80	−0.05	4.6044	2.25	2.27
25	74.991	6.58	−1.15	114.81	2.23	−0.56	6.2095	0.40	0.36
26	74.892	−1.03	−0.73	88.854	−0.75	−0.53	0.47409	−0.54	−0.27
27	67.381	−1.04	−1.46	98.015	−8.06	0.25	7.8266	0.79	0.42

[a] Cross-section of reference

[b] Relative error

Table 3 Material and number density in Case-A

Materials	Fuel rod			Clad	Moderator	
	^{235}U	^{238}U	^{16}O	Zr-Nat	H	^{16}O
Number density (10^{24}/cm^3)	4.21236E−04	2.26905E−02	4.62234E−02	3.89087E−02	4.42326E−02	2.21163E−02

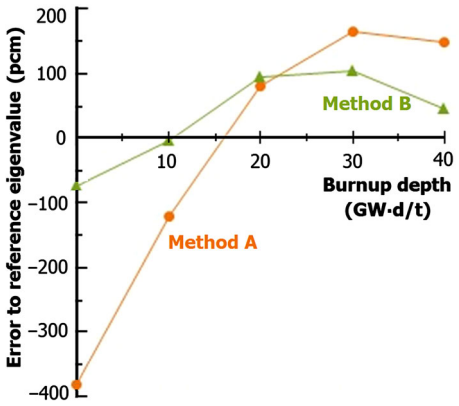

Fig. 3 Error in eigenvalue versus burnup

2. Perform fixed source transport calculation for each resonance group. The macroscopic total cross-section in resonance region is set to 100,000 (or any number that is large enough), and set to $\lambda \sum_{\mathrm{p}}$ for regions without resonance nuclide. The neutron source is set to $\lambda \sum_{\mathrm{p}}$ for all regions. The transport equation, Eq. (25), is solved with the MOC (method of characteristics):

$$\nabla \cdot \Omega \Psi_g(r,\Omega) = \sum_{\mathrm{t,g}} \Psi(r,\Omega) = \lambda \sum_{\mathrm{p,g}}, \tag{25}$$

where $\sum_{\mathrm{t,g}} = 10^5$ in resonance region and $\sum_{\mathrm{t,g}} = \lambda \sum_{\mathrm{p,g}}$ in non-resonance region. With the solution for the fixed source transport solution, the total reaction rate for each resonance region is calculated.

3. Dancoff factor for each resonance region in each resonance group is calculated through Eq. (15). And parameter A is calculated through Eq. (18).

4. In resonance regions and for resonance nuclides, the effective cross-section is calculated through Eq. (10).

5. For resonance nuclide other than ^{238}U, the effective cross-section is corrected by Eq. (23). For ^{238}U, the effective cross-section is corrected by Eq. (24).

3 Verification results

Numerical verifications were carried out for cases in lattice geometry, cases with two absorbers in the resonance region, and cases with multiple absorbers in the resonance region. To assess the effect coming separately from the Dancoff factor or the RIF, two calculations were performed for each case problem. As shown in Table 1.

Method A used the background cross-section iteration for resonance interference and Method B used the RIF table for resonance interference. Both methods used improved Dancoff factor in Stamm'ler equations. Method

Table 4 Material and number density in Case-B at burnup depth of 30 GW d/t

Materials	Fuel rod							Clad	Moderator	
	^{235}U	^{236}U	^{238}U	^{239}Pu	^{240}Pu	^{241}Pu	^{242}Pu	^{16}O	Zr-Nat	H	^{16}O
N^{a}	2.115×10^{-2}	8.449×10^{-3}	2.166	1.505×10^{-2}	4.441×10^{-3}	2.833×10^{-3}	7.811×10^{-4}	4.581	3.891	4.423	2.212

[a] Number density in $10^{22}/\mathrm{cm}^3$

Table 5 Micro-cross-section and relative error in absorption and neutron production for U and Pu in Case-B at burnup of 30 GW d/t

Energy groups	Absorption of ^{235}U			Neutron production of ^{235}U			Absorption of ^{236}U		
	$\sum$[a]	δ (%)[b]		$\sum$[a]	δ (%)[b]		$\sum$[a]	δ (%)[b]	
		Method A	Method B		Method A	Method B		Method A	Method B
15	4.4903	0.04	0.03	7.9297	0.06	0.05	1.0488	−1.51	−1.53
16	5.6829	−0.11	−0.09	10.421	−0.12	−0.09	1.2468	−1.65	−1.66
17	6.9896	−0.22	−0.16	12.588	−0.21	−0.21	1.5081	−1.75	−1.77
18	9.5685	−0.07	0.13	14.996	−0.37	0.06	1.9279	−2.88	−2.39
19	12.188	−0.65	−0.08	19.419	−1.06	−0.07	2.7944	−2.97	−1.95
20	16.959	−0.13	0.30	28.924	−0.06	0.49	5.0874	−4.49	−2.60
21	27.983	−0.28	−1.03	45.859	−0.97	−0.71	6.0751	−5.57	−9.20
22	34.903	−0.30	−0.17	53.623	0.05	−0.39	17.340	−7.43	−3.49
23	59.000	−2.68	0.11	100.37	−3.04	0.15	17.684	−11.6	−5.61
24	70.387	−3.19	0.06	104.40	−2.49	0.16	38.844	−14.2	−5.53
25	77.462	5.97	−1.77	118.40	1.62	−1.22	0.0511	−2.98	−1.28
26	78.153	−2.13	−1.86	91.932	−1.95	−1.77	0.1365	−1.10	−1.46
27	70.004	−1.65	−1.81	103.76	−10.13	−1.64	208.25	−4.97	−2.09

Energy groups	Absorption of ^{239}Pu			Neutron production of ^{239}Pu			Absorption of ^{238}U		
	$\sum$	δ (%)		$\sum$	δ (%)		$\sum$	δ (%)	
		Method A	Method B		Method A	Method B		Method A	Method B
15	3.6384	−0.01	−0.02	6.1712	−0.04	−0.04	69.268	−0.23	−0.20
16	4.5680	0.08	0.04	7.1936	0.11	0.08	0.7303	−0.87	−0.83
17	6.1122	−0.18	0.11	9.8722	0.14	0.41	0.9418	−1.70	−1.61
18	7.2395	−0.01	−0.46	10.503	0.55	−0.56	0.8698	−1.61	−1.53
19	10.240	3.16	−0.51	17.738	3.53	−0.59	1.1610	−1.82	−1.68
20	14.618	−2.45	0.34	24.590	−1.91	0.66	1.3305	−2.41	−2.19
21	29.322	−1.82	−3.08	44.010	−1.14	−1.64	1.5170	−0.02	0.06
22	49.759	−1.95	−1.14	85.083	−2.36	−1.34	2.3971	−0.26	0.18
23	100.02	4.41	−2.72	177.93	5.57	−2.95	2.0807	0.10	1.15
24	37.159	−9.15	0.90	29.986	−8.77	0.31	4.5449	2.19	2.71
25	79.071	−8.77	−0.89	122.97	−8.99	−1.21	6.1062	0.60	0.76
26	217.05	−1.83	−1.56	396.23	−2.03	−1.83	0.4759	−0.94	−0.10
27	54.238	−14.30	−2.16	89.712	−13.35	−2.55	7.8411	−0.11	0.95

[a] Cross-section of reference

[b] Relative error

C used the traditional Stamm'ler's method with the background cross-section iteration for resonance interference as a contrast. Together with verification for the case of non-lattice single assembly geometry, all calculations used the 69-groups WIMS-D format micro-library. For all the cases, continuous energy Monte Carlo calculation [10] was taken as the reference solution. Both the 69-group micro-nuclear data library and the continuous energy nuclear data library were used in all calculations, and verifications were developed from the basic library: ENDF/B-VII.0. Errors of eigenvalue in the verification results are all expressed in pcm, defined as ($x-$ reference) $\times 10^5$, where x is given by the tested method.

3.1 Infinite lattice cases

An infinite lattice of hexagonal fuel cells, as shown in Fig. 1, was used in the lattice calculation. Each side of the hexagonal cell is 7.83 mm. In the cell, the fuel rod is of 7.862 mm diameter, the clad made of Zr-Nat is 0.649 mm thick, and the moderator is light water at 300 K in both resonance and non-resonance regions.

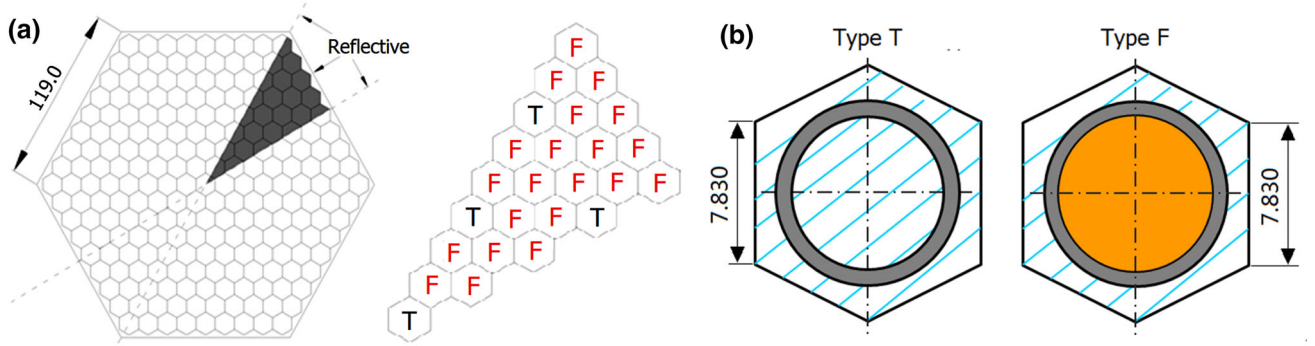

Fig. 4 Description of the assembly and arrangement of cells (**a**) and the cell types (**b**). *F* stands for fuel, and *T* stands for guide tube

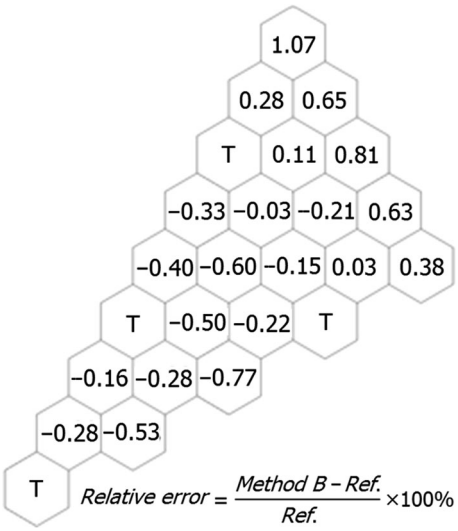

Fig. 5 Relative error of pin power in the assembly case

3.1.1 *Infinite lattice case with two resonance absorbers*

Let the fuel rod contain only UO_2, with ^{235}U enrichment of 0.8–3.6 % in steps of 0.2 %. Figure 2 shows errors of the eigenvalue as a function of the ^{235}U enrichment. One sees that Method A differs little from Method C. This indicates that our goal to find an alternative way to use Stamm'ler equations without possibility calculation is achieved. As Methods A and C have almost the same result, the following discussions will focus on Methods A and B.

There is a significant improvement in eigenvalue for Method B over Method A. This shows that the RIF table works much better than the background cross-section iteration in capturing resonance interference. The error of using Method B is around 100 pcm, which is quite acceptable in practice.

The verification results of 1.8 % enrichment, as a typical case named as Case-A for the convenience of discussion, are given in Table 2. Table 3 shows the nuclide composition in Case-A. The reference eigenvalue at 1.8 % enrichment is 1.22667 ± 0.00009 and the errors to the reference eigenvalue are -290 and -115 pcm (Fig. 2), for Methods A and B, respectively. From the microscopic cross-section for absorption and neutron production by each resonance nuclide (Table 2), one sees that the interference effect is mostly on ^{235}U, not on ^{238}U, as the Method B results are almost the same as the Method A results for ^{238}U. This is expected because of the large ^{238}U number density versus the much smaller number density of ^{235}U.

3.1.2 *Infinite lattice case with multiple resonance absorbers*

As the fuel burns, different resonance nuclides build up. A fresh UO_2 fuel with 3.1 % enrichment of ^{235}U is taken as an example to verify the proposed method at different burnup steps. Figure 3 shows the error in eigenvalue versus burnup of $10 - 40$ GW d/t using Method A or Method B to model the case. It can be seen that the RIF table captures the interference effect much better than the background cross-section iteration method, and the Method B results are quite acceptable.

The verification results are given in Tables 4 and 5 for 30 GW d/t burnup, as a particular case named as Case-B for the convenience of discussion. Table 4 shows the material and number density of nuclides, and Table 5 shows the effective cross-sections for major absorbers (^{235}U, ^{238}U, and ^{238}Pu). Again, Method B gives better performance than Method A in most cases for all nuclides except for ^{238}U. ^{238}U is almost not affected by resonance interference due to its very large number density. Therefore, the ^{238}U effective cross-section is not sensitive to using Method A or Method B. These results are consistent with those in Sect. 3.1.1.

4 The single assembly case

A hexagonal single assembly case is tested to verify the proposed method for non-lattice geometry. Figure 4a shows the whole assembly and the sector of one twelfth of the assembly with reflective boundary condition. The arrangement of the cells in the selected sector is shown on the right part of Fig. 4a. The cell types are shown in Fig. 4b. Type T cell is the guide tube cell filled with moderator and clad tube. Type F cell is the fuel cell filled with the fuel rod, clad tube, and moderator. As this is a rough assembly model, Types T and F cells share the same clad tube size and structure shown in Fig. 1. All fuel rods contain UO_2 of 1.8 % enrichment.

This single assembly problem was solved using Method B, and the results were compared to those of continuous energy Monte Carlo calculation for both eigenvalue and pin power distribution. The eigenvalue value is 1.24894 ± 0.00009, the error is -161 pcm, and the pin power distribution error is 1 % (Fig. 5). It should be noted that for this non-lattice problem, the Dancoff factor calculated with the neutron current method is position dependent, different for every fuel pin.

5 Conclusion

Incorporating the Dancoff factor into the Stamm'ler equations and evaluating the Dancoff factor by the neutron current method provide a convenient method to calculate the effective resonant cross-section. Not only it is easier to do the calculation but the validity is also generalized to non-lattice geometry. To correct for the resonance interference effect, a simplified RIF table can be used adequately. Test problems using the proposed method have shown very good results for both the lattice geometry case and the non-lattice geometry case. The use of RIF table is much better than the conventional background cross-section iteration method for resonance interference correction.

Acknowledgments The authors are very grateful to Dr. Yung-An Chao and Dr. Shao-Hong Zhang for their advice and supports.

References

1. R.J.J. Stamm'ler, M.J. Abbate, *Methods of Steady-State Reactor Physics in Nuclear Design* (Academic Press, London, 1983)
2. Y. Yamamoto, Stamm'ler's method for a heterogeneous lattice system, in *Handbook of Nuclear Engineering*, ed. by D.G. Cacuci (Springer, New York, 2010), pp. 1020–1023
3. N. Sugimura, A. Yamamoto, Evaluation of Dancoff factors in complicated geometry using the method of characteristics. J. Nucl. Sci. Technol. **43**, 1182–1187 (2006). doi:10.1080/18811248.2006.9711210
4. Y. Han, X.F. Jiang, D.Z. Wang, CMFD and GPU acceleration on method of characteristics for hexagonal cores. Nucl. Eng. Des. **280**, 210–222 (2014). doi:10.1016/j.nucengdes.2014.09.038
5. R.J.J. Stamm'ler, M.J. Abbate, *Methods of Steady-State Reactor Physics in Nuclear Design* (Academic Press, London, 1983)
6. J.R. Askew, F.J. Fayers, P.B. Kemshell, A general description of the lattice code WIMS. J. Br. Nucl. Energy Soc. **5**, 546–585 (1966)
7. Y. Yamamoto, Resonance interference factor (RIF) table, in *Handbook of Nuclear Engineering*, ed. by D.G. Cacuci (Springer, New York, 2010), pp. 1062–1063
8. S.T. Peng, X.F. Jiang, S.H. Zhang et al., Subgroup method with resonance interference factor table. Ann. Nucl. Energy. **59**, 176–189 (2013)
9. F. Leszczynski, Neutron resonance treatment with details in space and energy for pin cells and rod clusters. Ann. Nucl. Energy **14**, 589–601 (1987)
10. Z.F. Luo, R. Qiu, M. Li et al., Study of a GPU-based parallel computing method for the Monte Carlo program. Nucl. Sci. Tech. **25**(S1), S010501 (2014). doi:10.13538/j.1001-8042/nst.25.S010501